

## Flexural wave motion in viscous fluid: Stability analysis

Harekrushna Behera<sup>1</sup>, Siluvai Antony Selvan<sup>1</sup>, Sukhendu Ghosh<sup>2</sup> and Michael H. Meylan<sup>3</sup>

<sup>1</sup>Department of Mathematics, SRM Institute of Science and Technology, Kattankulathur 603203, Tamil Nadu, India.

<sup>2</sup>Department of Mathematics, Indian Institute of Technology, Jodhpur 342037, Rajasthan, India.

<sup>3</sup>School of Mathematical and Physical Sciences, University of Newcastle, NSW 2308, Australia.

E-mail: [hkb.math@gmail.com](mailto:hkb.math@gmail.com); [antony.selvan22@gmail.com](mailto:antony.selvan22@gmail.com); [sukhendu.math@gmail.com](mailto:sukhendu.math@gmail.com);  
[mike.meylan@newcastle.edu.au](mailto:mike.meylan@newcastle.edu.au)

### Highlights

- The flexural flow in the viscous fluid is studied using the linear stability analysis.
- The dynamical equation governing the infinite floating ice floe is obtained from the Euler–Bernoulli beam equation. Further, the fluid flow is governed by the two-dimensional Navier–Stokes equations, which are converted into the Orr–Sommerfeld system using the boundary conditions.
- A spectral collocation method is employed to solve the resultant Orr–Sommerfeld system.
- The study suggests that the floating ice floe incite the instability of viscous fluid flow. Thus, this method helps to perceive the dynamics of a floating elastic plate in the viscous fluid.

## 1 Introduction

The wave dynamics in the Marginal Ice Zone (MIZ) has been the subject of intensive research in recent decades. Experimental studies have shown the significance of ice floes on ocean wave propagation, but they lack a theoretical foundation<sup>[1]</sup>. Later, many studies developed theoretical explanations for the observed experimental facts<sup>[2]</sup>. Although such studies work well to explain the fluid flow through the MIZ and its wave attenuation phenomenon, there is still a need for accurate models which incorporate the viscosity of the fluid, which is neglected in the almost all previous studies. Simultaneously there has been a parallel interest in the stability analysis of flow systems in the past few decades<sup>[3]</sup>. Such a theory is applied in the chemical industries, biomedical engineering and the coating industries. Here the hydrodynamic instability is utilized in order to understand the stability of the flow system<sup>[4]</sup>. The instability of both gravity-driven and shear-driven free surface flow down an inclined plane was performed by Chin *et al.* <sup>[5]</sup>. Eventually, this method was implemented to study the characteristics of free surface flow controlled using the soluble<sup>[6]</sup> and insoluble<sup>[7]</sup> surfactants. It was observed that these surfactants could control the surface-elasticity of the free surface. In the proposed study, the viscous fluid is considered, and the structural parameters of the elastic plate are incorporated in the tangential stress balance. This study allows us to understand the flexural wave motion in viscous fluid better. From the physical viewpoint, the present study can be employed to understand the attenuation of waves by ice floes in MIZ.

## 2 Mathematical formulation

The problem is studied in the two-dimensional Cartesian coordinate system with the infinitely extended ice sheet on the mean free surface  $z = h$ . The Newtonian fluid flow is considered as incompressible and irrotational with the direction of flow along the positive  $x$ -axis, and the positive  $z$ -axis is pointing upward from the origin  $O$ . The bottom is considered as rigid, whereas the deflection of ice sheet on the surface is denoted as  $z = \eta(x, t)$ . The dimensionless equations governing the fluid flow beneath the ice sheet are given by the two-dimensional Navier–Stokes equations

$$\partial_x u + \partial_z w = 0, \quad (1)$$

$$\partial_t u + u \partial_x u + w \partial_z u = -\partial_x p + \frac{1}{Re} \nabla^2 u, \quad (2)$$

$$\partial_t w + u \partial_x w + w \partial_z w = -\partial_z p + \frac{1}{Re} \nabla^2 w - G, \quad (3)$$

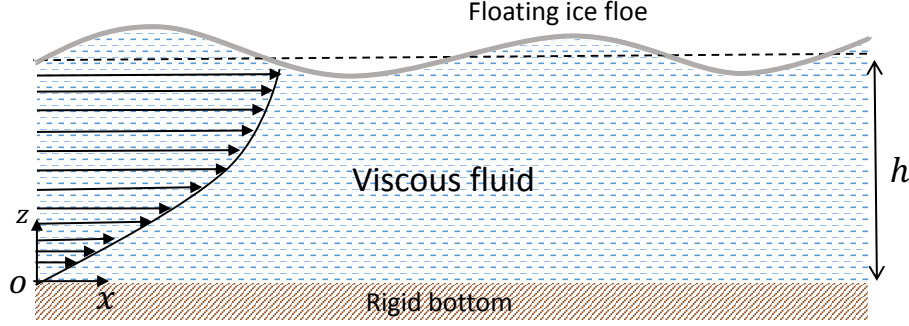


Figure 1: Schematic sketch of fluid flow under the infinite extended floating ice-sheet in viscous fluid

where  $p$  be the pressure inside fluid flow,  $u$  and  $w$  are the horizontal and vertical components of the velocity, respectively. Further, non-dimensional form of the acceleration due to gravity is given by  $G = gh/U^2$ , where  $g$  and  $h$  are the acceleration due to gravity and mean free surface, respectively. Moreover, the characteristic velocity scale is denoted as  $U = gh^2/\nu$  with  $\nu$  being the kinematic viscosity of fluid. At ice-covered surface, the kinematic condition along with the tangential and normal stress balance conditions are given by

$$w = \partial_t \eta + u \partial_x \eta \quad \text{for } z = \eta(x, t), \quad (4)$$

$$(\partial_z u + \partial_x w)(1 - (\partial_x \eta)^2) - 4 \partial_x u \partial_x \eta = 0 \quad \text{for } z = \eta(x, t), \quad (5)$$

$$\begin{aligned} Re p = \frac{2}{1 + (\partial_x \eta)^2} \{ (\partial_x u)(\partial_x \eta)^2 - (\partial_z u + \partial_x w) \partial_x \eta + \partial_z w \} + \bar{\alpha} \frac{\partial^2}{\partial x^2} \frac{\partial_{xx}^2 \eta}{(1 + (\partial_x \eta)^2)^{3/2}} \\ + \bar{\beta} \frac{\partial_{xx}^2 \eta}{(1 + (\partial_x \eta)^2)^{3/2}} - \bar{\gamma} Re \partial_{tt}^2 \eta \quad \text{for } z = \eta(x, t), \end{aligned} \quad (6)$$

where  $\bar{\alpha} = EI/\rho gh^4$ ,  $\bar{\beta} = N/\rho gh^2$ , and  $\bar{\gamma} = m_p/\rho h$  are the non-dimensional form of the structural rigidity, compressive force and mass per unit length, respectively with  $\rho$  is the density of fluid. It is assumed that sea bottom is rigid, thus the boundary condition is given by

$$u = 0 \quad \text{and} \quad w = 0 \quad \text{for } z = 0. \quad (7)$$

The base state of the fully developed flow is obtained by considering  $\vec{v} = (u_B(z), 0)$  and  $\vec{p} = (p_B(z), 0)$ , where  $u_B(z)$  and  $p_B(z)$  be the base state of velocity and pressure, respectively. By solving the equations (2)–(3) along with the boundary conditions (4)–(7) using the above vectorial notation, yield the following solution

$$u_B(z) = \tanh(2z), \quad (8)$$

$$p_B(z) = G(1 - z). \quad (9)$$

In the case of velocity base profile (as in Eq. (8)), it is approximated using the tangent hyperbolic function in order to impose the shear rate inside the flow. This, in turns, increases towards the surface. Now, the base state excited with the small disturbance using the perturbation technique. All the dynamical variables are represented as follow

$$u(x, z, t) = u_B(z) + \tilde{u}(x, z, t), \quad (10a)$$

$$w(x, z, t) = \tilde{w}(x, z, t), \quad (10b)$$

$$p(x, z, t) = p_B(z) + \tilde{p}(x, z, t), \quad (10c)$$

$$\eta(x, t) = 1 + \tilde{\eta}(x, t), \quad (10d)$$

where  $\tilde{p}$ ,  $\tilde{\eta}$ ,  $\tilde{u}$  and  $\tilde{w}$  denote the perturbed pressure, deflection, horizontal and vertical velocities, respectively. Further, the perturbed velocity along the horizontal and vertical directions are defined

as  $\tilde{u} = \partial_z \psi$  and  $\tilde{w} = -\partial_x \psi$ , where  $\psi$  be the stream function. Using the normal mode analysis, the stream function and the perturbed deflection are given as,

$$\psi(x, z, t) = \phi(z) e^{ik(x-ct)} \quad \text{and} \quad \tilde{\eta}(x, z, t) = \zeta(z) e^{ik(x-ct)}, \quad (11)$$

where  $c$  and  $k$  be the complex-valued wave speed and wavenumber, respectively. Expressing the governing equations (1)–(3) along with the boundary conditions (4)–(7) using the (10)–(11) yield the following Orr-sommerfeld system

$$(d_z^2 - k^2)^2 \phi - ikRe[(d_z^2 - k^2)(u_B - c) - d_z^2 u_B] \phi = 0, \quad (12)$$

$$d_z \phi = 0 \quad \text{and} \quad \phi = 0 \quad \text{for} \quad z = 0, \quad (13)$$

$$\phi + \zeta(u_B - c) = 0 \quad \text{for} \quad z = 1, \quad (14)$$

$$d_z^2 u_B \zeta + (d_z^2 + k^2) \phi = 0 \quad \text{for} \quad z = 1, \quad (15)$$

$$\begin{aligned} [d_z^3 - 3k^2 d_z - ikReu_B d_z + ikRed_z u_B] \phi + [-2ik - 2k^2 d_z u_B - \bar{\alpha} i k^5 + \bar{\beta} i k^3] \zeta \\ [ikRed_z - ik^3 Re \bar{\gamma}] (c\phi) - ik^3 \bar{\gamma} Re u_B (c\zeta) = 0 \quad \text{for} \quad z = 1, \end{aligned} \quad (16)$$

where  $d_z$  be the derivative with respect to  $z$ . It may be noted that for  $\bar{\alpha} \rightarrow 0$ ,  $\bar{\gamma} \rightarrow 0$  and  $\bar{\beta} = -\bar{\beta}_0 Re^{-2/3}$  with  $\bar{\beta}_0 = (\sigma/\rho)(2/g\nu^4)^{1/3}$  in (12)–(16) give the Orr-Sommerfeld system for the fluid flow having free surface with surface tension  $\beta$  (as in Chin *et al.* [5]).

### 3 Results and discussion

Here, the Orr-Sommerfeld system (12)–(16) is solved numerically using the spectral collocation method. Using the linear mapping technique, the physical interval  $[0, 1]$  is transformed into the computational interval  $[-1, 1]$  and discretized by the Chebyshev polynomial. After solving, the complex-valued eigenvalues  $c = c_r + ic_i$  are obtained for a certain wavenumber  $k$ . Further, the spatio-temporal growth rate is defined as  $\omega_i = kc_i$  with  $c_i$  being the imaginary part of  $c$ . The stability of fluid depends on the signs of  $\omega_i$ :  $\omega_i < 0$  (stable),  $\omega_i > 0$  (unstable) and  $\omega_i = 0$  (neutral). Apart from this, the deflection of ice floe and velocity flux of fluid under the ice sheet are analyzed. It is worth to be pointed that in the present physical model,  $\bar{\beta}$  behaves as compressive force on the ice floe. However, the external compressive force acting on the floating ice floe is neglected here.

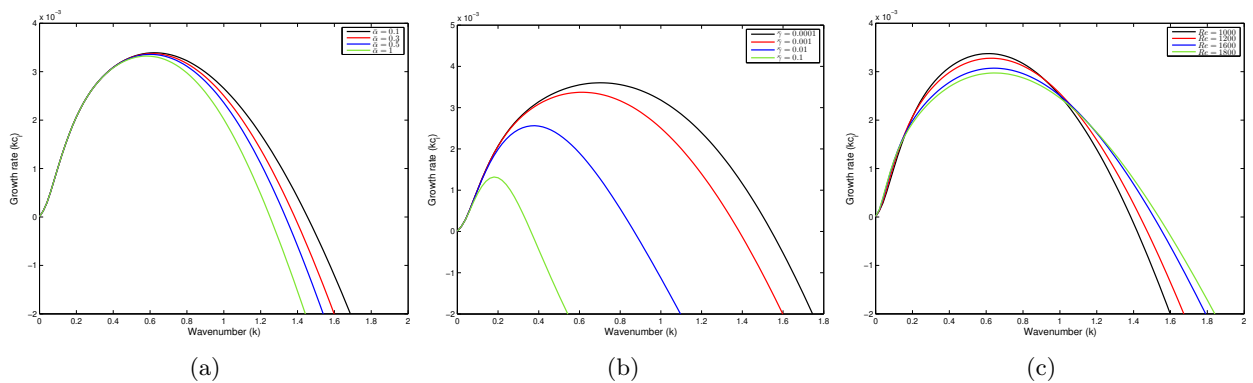


Figure 2: Growth rate  $kc_i$  against the wavenumber  $k$  for different values of (a) structural rigidity  $\bar{\alpha}$  with  $\bar{\gamma} = 0.001$  and  $Re = 1000$ , (b) mass per unit length  $\bar{\gamma}$  with  $\bar{\alpha} = 0.3$  and  $Re = 1000$ , and (c) Reynolds number  $Re$  with  $\bar{\alpha} = 0.3$  and  $\bar{\gamma} = 0.001$ .

In Figs. 2(a), (b) and (c), the spatio-temporal growth rate of the most unstable mode ( $kc_i$ ) is plotted as a function of wavenumber ( $k$ ) for different values of structural rigidity ( $\bar{\alpha}$ ), mass per unit length ( $\bar{\gamma}$ ) and Reynolds number ( $Re$ ), respectively. In general, the variation of growth rate against the wavenumber is two-fold (i.e., the growth rate initially increases and attains maximum value, then

decreases for an increase in the value of  $k$ ). Moreover, the parameters such as structural rigidity and mass per unit length have the stabilizing effect on the fluid flow (Figs. 2(a) and (b)), whereas the Reynolds number has a stabilizing effect till  $k \leq 1.2$  and destabilizing effect for the values of  $k > 1.2$ . On the other hand, in the case of Fig. 3, the horizontal velocity  $u$  in the fluid domain is compared for the both free surface (Fig. 3(a)) and plate-covered surface (Fig. 3(b)). In general, from both the figures, it is observed that the horizontal velocity increases at the surface for both the free surface and plate-covered surface. However, the velocity of fluid flow decreases in the presence of a floating elastic plate as compared to that for the free surface.

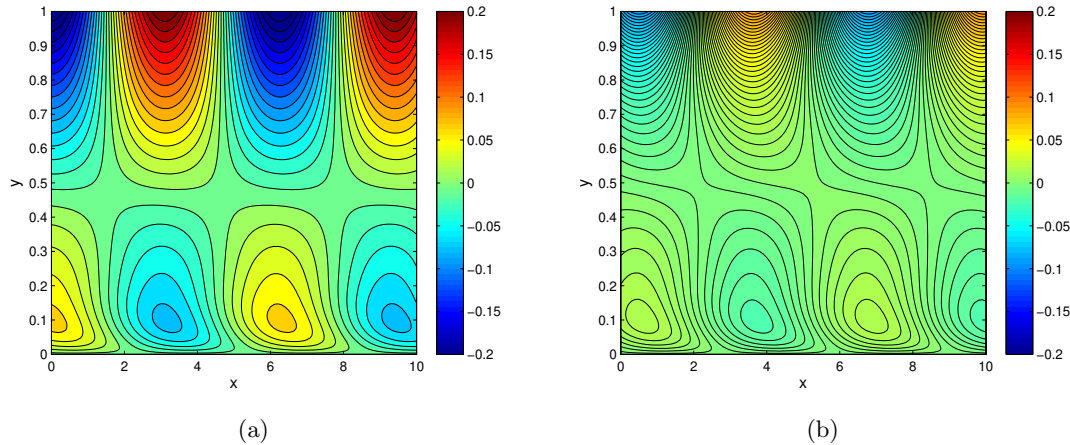


Figure 3: Distribution of the horizontal velocity  $u$  in the fluid domain for the (a) free surface ( $\bar{\alpha} = 0$ ,  $\bar{\gamma} = 0$ ,  $Re = 1000$  and  $\bar{\beta}_0 = 1200$ ), and (b) plate-covered surface ( $\bar{\alpha} = 0.3$ ,  $\bar{\gamma} = 0.001$ ,  $Re = 1000$  and  $\bar{\beta} = 0$ ).

**Further results will be presented in the workshop.**

### Acknowledgment

HB gratefully acknowledges the financial support from SERB, Department of Science and Technology, Government of India through “CRG” project, Award No. CRG/2018/004521.

### References

- [1] P. Wadhams, V. A. Squire, D. J. Goodman, A. M. Cowan, and S. C. Moore, *Journal of Geophysical Research: Oceans* **93**, 6799 (1988).
- [2] M. H. Meylan, *Journal of Geophysical Research: Oceans* **107**, 5 (2002).
- [3] C.-S. Yih, *Selected Papers By Chia-Shun Yih: (In 2 Volumes)* (World Scientific, 1991) pp. 522–526.
- [4] S. Ghosh and H. Behera, *ZAMM-Journal of Applied Mathematics and Mechanics/Zeitschrift für Angewandte Mathematik und Mechanik* **98**, 1947 (2018).
- [5] R. Chin, F. Abernath, and J. Bertshy, *Journal of Fluid Mechanics* **168**, 501 (1986).
- [6] A. Kalogirou and M. Blyth, *Journal of Fluid Mechanics* **873**, 18 (2019).
- [7] Anjalajah, R. Usha, and S. Millet, *Physics of Fluids* **25**, 022101 (2013).